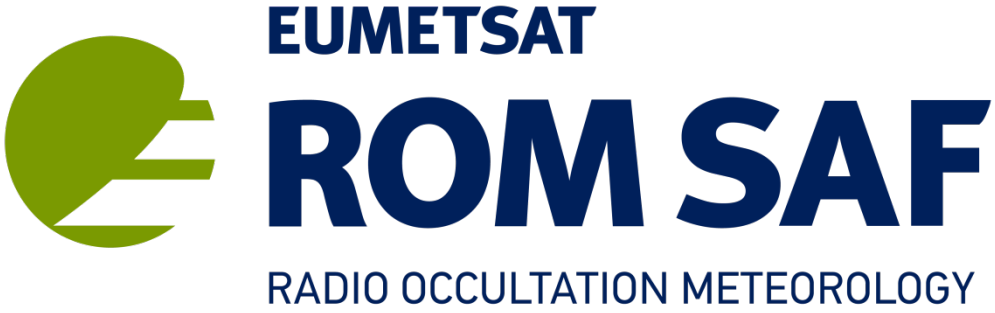

Algorithm Theoretical Baseline Document: Level 1B bending angles

Version 2.1

15 May 2020

ROM SAF Consortium
Danish Meteorological Institute (DMI)
European Centre for Medium-Range Weather Forecasts (ECMWF)
Institut d'Estudis Espacials de Catalunya (IEEC)
Met Office (METO)

Ref: SAF/ROM/DMI/ALG/BA/001

DOCUMENT AUTHOR TABLE

	Author(s)	*Function*	*Date*
Prepared by:	Stig Syndergaard	ROM SAF Design Coordinator	15/05/2020
Reviewed by (internal):	Hans Gleisner	ROM SAF Climate Coordinator	21/02/2020
Approved by:	Kent B. Lauritsen	ROM SAF Project Manager	15/05/2020

DOCUMENT CHANGE RECORD

Version	*Date*	*By*	*Description*
Draft	10/04/2013	KMK	Original draft
1.0	15/03/2016	SSY	Version for PCR-RE1 review. First version of ATBD for bending angles
1.1	12/08/2016	SSY	Updated version after PCR-RE1 review, taking into account RIDs #2, #8, #10, #12, #21, #22, #23, #24, #25, #28.
1.2	23/02/2017	SSY	Internal version. Updated version reflecting changes in processing codes, configuration parameters, and QC as a result of tests before reprocessing RE1: - Section 3.2.4: Changed threshold of BA cut-off. - Section 3.2.11: Changed Q_{L2} threshold to 25 instead of 15; changed range to 25-50 km instead of 15-50 km. These parameters are related to lowering the altitude of the L2-extrapolation in general and allowing Metop rising occultations to be nominal even when L2 data are missing up to 25 km. - Section 3.2.17: Added sentence about transition between GO and WO regions. - Section 3.2.18: Added sentence about transition between estimated and extrapolated L2 BA. - Section 4.2: Revised QC parameters and checks. - Removed Section 5.2.7 regarding kink at 25 km, which is now gone as a consequence of the change described in Section 3.2.17. - Removed Section 5.2.8 regarding kink due to L2-extrapolation, which is now gone as a consequence of the change described in Section 3.2.18. - Section 7.2: Added opt_XL2 in Section 5 of example configuration file.

1.3	11/06/2018	SSY	Version prepared for DRR-RE1 & ORR reviews. Updated version reflecting changes in pre-processing of GRAS data, as well as additions to the pre-processing of CHAMP and GRACE missions: - Section 1.2.2: Added [RD.27] to reference documents. - Section 3.2.1: Added sentence about transformation from J2000 to True-of-Date ECI. - Section 3.2.4: Added description of additional pre-processing for CHAMP and GRACE. - Section 3.2.5: Clarified the mission-dependent use of navigation bits. - Section 4.2: Added sentence that bending angle is marked as non-nominal if excess phase or refractivity is non-nominal. - Section 4.2: Added sentence about additional quality check at very high altitudes. - Section 7.2: Updated example configuration file. - Updated EUMETSAT logo.
1.4	31/08/2018	SSY	Updated version implementing the following RIDs from the DRR-RE1 & ORR review: - RIDs 021, 022, 023, 026, 027, 028, 029, 030, 031, 032, 033, 034, 036, 037, 038, 041, 042, 043, 044, 046, 070, 074, 194, 195, 196: Editorial/minor changes. In addition the following changes were made: - Included a few additional editorials provided by Barbara Scherllin-Pirscher.
1.5	20/12/2018	SSY	Updated version based on ICDR concept discussions at ROM SAF SG22: - Page 4: Update of the ROM SAF preface. - Table 1.1: Included ICDR products. - Section 1.4: New definitions of product types. - Section 6: Now referring to the new product types.
2.0	21/02/2020	SSY	Updated version for EPS-SG PDCR review: - Section 1.1: added Table 1.2 with EPG-SG products. - Section 1.1.1: New section on ROM SAF EPS-SG products. - Section 1.4: Modified NRT definitions for EPS-SG - Chapter 7: New chapter describing algorithm differences for EPS-SG products. Updated version for ORR12 review: - Table 1.1: Included GRM-66 (Metop-C) - Section 1.2.2: Added reference on residual ionospheric correction method [RD.31] - Section 3.1.1: Introduced f_1 and f_2 symbols for L1 and L2 frequencies - Section 3.2.20: Included brief description of residual ionospheric correction method. - Section 3.2: Added a footnote briefly noting that 50Hz SNRs for Metop are reconstructed from 1 kHz raw sampling data. - Section 3.3: Modified to include residual ionospheric correction. - Section 6: Updated to reflect new difference between offline and CDR/ICDR processing.

2.1	15/05/2020	SSY	Updated version implementing the following RIDs from the ORR12 review: - RIDs 043, 098: Section 1.1: Removed text about future EPS-SG Day 1 products - RIDs 043, 098: Removed Section 1.1.1 and Chapter 7 about future EPS-SG Day 1 products - RID 035: Added Section 1.5 giving an overview of the remainder of the document - RID 098: Section 3.1.4: Changed GPS to GNSS

ROM SAF

The Radio Occultation Meteorology Satellite Application Facility (ROM SAF) is a decentralised processing centre under EUMETSAT which is responsible for operational processing of radio occultation (RO) data from the Metop and Metop-SG satellites and radio occultation data from other missions. The ROM SAF delivers bending angle, refractivity, temperature, pressure, humidity, and other geophysical variables in near real-time for NWP users, as well as reprocessed Climate Data Records (CDRs) and Interim Climate Data Records (ICDRs) for users requiring a higher degree of homogeneity of the RO data sets. The CDRs and ICDRs are further processed into globally gridded monthly-mean data for use in climate monitoring and climate science applications.

The ROM SAF also maintains the Radio Occultation Processing Package (ROPP) which contains software modules that aid users wishing to process, quality-control and assimilate radio occultation data from any radio occultation mission into NWP and other models.

The ROM SAF Leading Entity is the Danish Meteorological Institute (DMI), with Cooperating Entities: i) European Centre for Medium-Range Weather Forecasts (ECMWF) in Reading, United Kingdom, ii) Institut D'Estudis Espacials de Catalunya (IEEC) in Barcelona, Spain, and iii) Met Office in Exeter, United Kingdom. To get access to our products or to read more about the ROM SAF please go to: http://www.romsaf.org

Intellectual Property Rights

List of Contents

1. Introduction

1.1 Purpose

This ATBD document describes the algorithms used to derive the offline and reprocessed bending angle products produced by the Radio Occultation Meteorology (ROM) Satellite Application Facility (SAF). The complete list of products covered by this ATBD is provided in Table 1.1[1]. Note that this table includes (or may include) both products in development and products with operational status. The status of all ROM SAF data products is available at the website: http://www.romsaf.org

The product requirements baseline is the PRD version 2.3 [AD.3]. The ATBD software package is based on the ROPP [RD.1].

Table 1.1 List of products covered by this ATBD

Product ID	Product name	Product acronym	Product type	Operational satellite input	Dissemination means	Dissemination format
GRM-08	Offline Bending Angle	OBAMEA	Offline Product	Metop-A Level 1A data from EUM Secretariat	Web	BUFR/netCDF
GRM-29-L1-B-R1	Reprocessed Bending Angle	RBAMET	Climate Data Record	Metop Level 1A data from EUM Secretariat	Web	BUFR/netCDF
GRM-29-L1-B-I1	ICDR Bending Angle	IBAMET	Interim Climate Data Record	Metop Level 1A data from EUM Secretariat	Web	BUFR/netCDF
GRM-30-L1-B-R1	Reprocessed Bending Angle	RBACO1	Climate Data Record	COSMIC Level 1A data from CDAAC	Web	BUFR/netCDF
GRM-32-L1-B-R1	Reprocessed Bending Angle	RBACHA	Climate Data Record	CHAMP Level 1A data from CDAAC	Web	BUFR/netCDF
GRM-33-L1-B-R1	Reprocessed Bending Angle	RBAGHA	Climate Data Record	GRACE Level 1A data from CDAAC	Web	BUFR/netCDF
GRM-46	Offline Bending Angle	OBAMEB	Offline Product	Metop-B Level 1A data from EUM Secretariat	Web	BUFR/netCDF
GRM-66	Offline Bending Angle	OBAMEC	Offline Product	Metop-C Level 1A data from EUM Secretariat	Web	BUFR/netCDF

[1] Detailed information on the different input data types and their version numbers can be found in the validation reports at www.romsaf.org/product_documents.php.

1.2 Applicable and reference documents

1.2.1 Applicable documents

The following list contains documents with a direct bearing on the contents of this document:

[AD.1] CDOP-3 Proposal: Proposal for the Third Continuous Development and Operations Phase (CDOP-3); Ref: SAF/ROM/DMI/MGT/CDOP3/001 Version 1.2 of 31 March 2016, Ref: EUM/C/85/16/DOC/15, approved by the EUMETSAT Council at its 85th meeting on 28-29 June 2016

[AD.2] CDOP-3 Cooperation Agreement: Agreement between EUMETSAT and DMI on the Third Continuous Development and Operations Phase (CDOP-3) of the Radio Occultation Meteorology Satellite Applications Facility (ROM SAF), Ref. EUM/C/85/16/DOC/19, approved by the EUMETSAT Council and signed at its 86th meeting on 7 December 2016

[AD.3] ROM SAF Product Requirements Document, Ref. SAF/ROM/DMI/MGT/PRD/001

1.2.2 Reference documents

The following documents provide supplementary or background information, and could be helpful in conjunction with this document:

[RD.1] The Radio Occultation Processing Package (ROPP) User Guide, Part III: Pre-processor module, Ref. SAF/ROM/METO/UG/ROPP/004

[RD.2] Gorbunov ME (2009) Upgrading of OCC code for operational processing of GRAS raw sampling data. ROM SAF CDOP Visiting Scientist Report 6, Ref: SAF/GRAS/DMI/MGT/CVS06/003

[RD.3] Bonnedal M, Christensen J, Carlström A, Berg A (2010) Metop-GRAS in-orbit instrument performance. GPS Solutions 14:109-120, doi:10.1007/s10291-009-0142-3

[RD.4] Gorbunov ME, Kornblueh L (2003) Principles of variational assimilation of GNSS radio occultation data. Report No. 350, Max-Planck-Institute for Meteorology, Hamburg, Germany

[RD.5] Zus, F, et al. (2011) Validation of refractivity profiles derived from GRAS raw-sampling data. Atmos. Meas. Tech. 4:1541-1550, doi:10.5194/amt-4-1541-2011

[RD.6] Hedin AE (1991) Extension of the MSIS thermosphere model into the middle and lower atmosphere. J. Geophys. Res. 96:1159-1172

[RD.7] Gorbunov ME, Shmakov AV, Leroy SS, Lauritsen KB (2011) COSMIC radio occultation processing: Cross-center comparison and validation. J Atmos Ocean Technol 28:737–751.

[RD.8] Kursinski ER, Hajj GA, Schofield JT, Linfield RP, Hardy KR (1997) Observing Earth's atmosphere with radio occultation measurements using the Global Positioning System. J Geophys Res 102:23429–23465

[RD.9] Gorbunov ME, Lauritsen KB, Rhodin A, Tomassini M, Kornblueh L (2006) Radio holographic filtering, error estimation, and quality control of radio

occultation data. J. Geophys. Res. 111:D10105, doi:10.1029/2005JD006427

[RD.10] Gorbunov ME, Lauritsen KB (2004) Analysis of wave fields by Fourier integral operators and their application for radio occultations. Radio Sci 39:RS4010, doi:10.1029/2002RS002971

[RD.11] Syndergaard S (2012) Deriving bending angle, refractivity, temperature, and pressure using GRAS SAF software. Technical report (WP-2) of Assessment of the Structural Uncertainty of GRAS Products from Level 1B (bending angles) up to Level 2 (temperatures), Danish Meteorological Institute, EUMETSAT Contract No. EUM/CO/10/4600000745/AvE.

[RD.12] Gorbunov ME (2002) Canonical transform method for processing radio occultation data in the lower troposphere. Radio Sci. 37:1076, doi:10.1029/2000RS002592

[RD.13] Foelsche, U, Syndergaard S, Fritzer J, and Kirchengast G (2011) Errors in GNSS radio occultation data: relevance of the measurement geometry and obliquity of profiles. Atmos Meas Tech 4:189-199, doi:10.5194/amt-4-189-2011

[RD.14] Algorithm Theoretical Baseline Document: Level 2A refractivity profiles, Ref. SAF/ROM/DMI/ALG/REF/001

[RD.15] Algorithm Theoretical Baseline Document: Level 2A dry temperature profiles, Ref. SAF/ROM/DMI/ALG/TDRY/001

[RD.16] The Radio Occultation Processing Package (ROPP) User Guide, part I: Input/Output module, Ref. SAF/ROM/METO/UG/ROPP/002

[RD.17] WMO FM94 (BUFR) Specification for Radio Occultation Data, Ref. SAF/ROM/METO/FMT/BUFR/001

[RD.18] Healy SB., Eyre JR, Hamrud M and Thépaut, J-N (2007) Assimilating GPS radio occultation measurements with two-dimensional bending angle observation operators. Q.J.R. Meteorol. Soc., 133: 1213–1227. doi: 10.1002/qj.63

[RD.19] Gorbunov ME, Lauritsen KB (2009) Error estimate of bending angles in the presence of strong horizontal gradients. In New Horizons in Occultation Research, edited by A Steiner et al, pp 17-26, Springer Verlag, doi:10.1007/978-3-642-00321-9_2

[RD.20] Lauritsen KB, Syndergaard S, Gleisner H, Gorbunov ME, Rubek F, Sørensen MB, Wilhelmsen H (2011) Processing and validation of refractivity from GRAS radio occultation data. Atmos. Meas. Tech. 4:2065-2071, doi:10.5194/amt-4-2065-2011

[RD.21] Syndergaard S (2012) Assessment of the Structural Uncertainty of GRAS Products from Level 1B (bending angles) up to Level 2 (temperatures), Final Report, Danish Meteorological Institute, EUMETSAT Contract No. EUM/CO/10/4600000745/AvE.

[RD.22] Zeng Z, Sokolovskiy S (2010) Effect of sporadic E clouds on GPS radio occultation signals. Geophys Res Lett 37:L18817, doi:10.1029/2010GL044561

[RD.23] Sokolovskiy SV (2001) Tracking tropospheric radio occultation signals from low Earth orbit. Radio Sci 36:483-498

[RD.24] Sokolovskiy SV, Schreiner W, Rocken C, and Hunt D (2009) Optimal noise filtering for the ionospheric correction of GPS radio occultation signals. J. Atmos. & Oceanic Tech. 26:1398-1403, doi:10.1175/2009JTECHA1192.1

[RD.25] Kinch KM, Lauritsen KB, Gorbunov ME, Wilhelmsen H (2011) Processing of GRAS raw sampling data. In Proceedings WPP 236 of the 3rd International Colloquium – Scientific and Fundamental Aspects of the Galileo Programme, 31

August – 2 September, 2011, Copenhagen, Denmark, 8 pp.

[RD.26] Gorbunov ME, Lauritsen KB, Rhodin A, Tomassini M, Kornblueh L (2006) Radio holographic filtering and error estimation of radio occultation data. In Proceedings of 3rd ESA Workshop on Satellite Navigation User Equipment Technologies – NAVITEC, 11-13 December, 2006, ESTEC, Netherlands, 8 pp.

[RD.27] Hoffman-Wellenhof B, Lichtenegger H, Wasle E (2008) GNSS – Global Navigation Satellite Systems: GPS, GLONASS, Galileo & more. Springer Wien New York, 516 pp.

[RD.28] Syndergaard S (2013) Assessment of ionospheric corrections. Technical note (WP1100) of Potentials for Radio Occultations with Future Galileo Frequencies, Danish Meteorological Institute, ESA Contract No. 4000103330/11/NL/CV, European GNSS Evolution Programme.

[RD.29] Ho SP, et al. (2012) Reproducibility of GPS radio occultation data for climate monitoring: Profile-to-profile inter-comparison of CHAMP climate records 2002 to 2008 from six data centers. J. Geophys. Res. 117:D18111, doi:10.1029/2012JD017665

[RD.30] Steiner AK, et al. (2013) Quantification of structural uncertainty on climate data records from GPS radio occultation. Atmos. Chem. Phys. 13:1469-1484, doi:10.5194/acp-13-1469-2013

[RD.31] Healy SB, Culverwell, ID (2015) A modification to the standard ionospheric correction method used in GPS radio occultation. Atmos. Meas. Tech. 8:3385-3393, doi:10.5194/amt-8-3385-2015

1.3 Acronyms and abbreviations

ATBD	Algorithm Theoretical Baseline Document
BA	Bending Angle
BAROCLIM	Bending Angle Radio Occultation Climatology
BUFR	Binary Universal Format for data Representation
CDAAC	COSMIC Data Analysis and Archival Center
CDOP	Continuous Development and Operations Phase
CDR	Climate Data Record
CHAMP	Challenging Mini-satellite Payload
CL	Closed Loop
COSMIC	Constellation Observing System for Meteorology, Ionosphere, and Climate
CT	Canonical Transform
CT2	CT of the second kind
DMI	Danish Meteorological Institute
ECF	Earth Centered Fixed
ECI	Earth Centered Inertial
ECMWF	European Centre for Medium-range Weather Forecasts
EGM96	Earth Gravitational Model
EPS	EUMETSAT Polar satellite System
EGS-SG	EPS Second Generation

EUMETSAT	EUropean organisation for the exploitation of METeorological SATellites
FIO	Fourier Integral Operator
GMST	Greenwich Mean Sidereal Time
GNSS	Global Navigation Satellite System
GO	Geometric Optics
GPS	Global Positioning System (US)
GRACE	Gravity Recovery and Climate Experiment
GRAS	GNSS Receiver for Atmospheric Sounding (Metop instrument)
ICDR	Interim Climate Data Record
IEEC	Institut d'Estudis Espacials de Catalunya (Spain)
ITOE	Inertial True-of-Epoch
LEO	Low Earth Orbit
Metop	Meteorological Operational Polar satellite (EPS/EUMETSAT)
MSIS	Mass Spectrometer and Incoherent Scatter
NCO	Numerically Controlled Oscillator
NetCDF	Network Common Data Form
NRT	Near Real-Time
NWP	Numerical Weather Prediction
OL	Open Loop
PRD	Product Requirements Document
PP	Pre-Processor
QC	Quality Control
RMS	Root Mean Square
RO	Radio Occultation
ROM SAF	Radio Occultation Meteorology SAF (EUMETSAT), former GRAS SAF
ROPP	Radio Occultation Processing Package
RS	Raw Sampling
SAF	Satellite Application Facility (EUMETSAT)
SLTP	Straight-Line Tangent Point
SNR	Signal-to-noise ratio
UCAR	University Corporation for Atmospheric Research
WMO	World Meteorological Organisation
WO	Wave Optics

1.4 Definitions

RO data products from the Metop and Metop-SG satellites and RO data from other missions are grouped in *data levels* (level 0, 1, 2, or 3) and *product types* (NRT, offline, CDR, or ICDR). The data levels and product types are defined below[2]. The lists of

[2]Note that the level definitions differ partly from the WMO definitions: http://www.wmo.int/pages/prog/sat/dataandproducts_en.php

variables should not be considered as the complete contents of a given data level, and not all data may be contained in a given data level.

Data levels:

Level 0: Raw sounding, tracking and ancillary data, and other GNSS data before clock correction and reconstruction;

Level 1A: Reconstructed full resolution excess phases, total phases, pseudo ranges, SNRs, orbit information, I, Q values, NCO (carrier) phases, navigation bits, and quality information;

Level 1B: Bending angles and impact parameters, tangent point location, and quality information;

Level 2: Refractivity, geopotential height, "dry" temperature profiles (Level 2A), pressure, temperature, specific humidity profiles (Level 2B), surface pressure, tropopause height, planetary boundary layer height (Level 2C), ECMWF model level coefficients (Level 2D), quality information;

Level 3: Gridded or resampled data, that are processed from Level 1 or 2 data, and that are provided as, e.g., daily, monthly, or seasonal means on a spatiotemporal grid, including metadata, uncertainties and quality information.

Product types:

NRT product: Data product delivered less than: (i) 3 hours after measurement (ROM SAF Level 2 for EPS); (ii) 150 min after measurement (ROM SAF Level 2 for EPS-SG Global Mission); (iii) 125 min after measurement (ROM SAF Level 2 for EPS-SG Regional Mission);

Offline product: Data product delivered from less than 5 days to up to 6 months after measurement, depending on the requirements. The evolution of this type of product is driven by new scientific developments and subsequent product upgrades;

CDR: Climate Data Record generated from a dedicated reprocessing activity using a fixed set of processing software[3]. The data record covers an extended time period of several years (with a fixed end point) and constitutes a homogeneous data record appropriate for climate usage;

ICDR: An Interim Climate Data Record (ICDR) regularly extends in time a (Fundamental or Thematic) CDR using a system having optimum consistency with and lower latency than the system used to generate the CDR[4].

1.5 Overview of this document

Chapter 2 gives a short algorithm overview, and Chapter 3 describes the technical details. Practical considerations such as validation method and quality control is given in Chapter 4, whereas assumptions and limitations are discussed in Chapter 5. Differences for NRT, offline, CDR, and ICDR products are described in Chapter 6.

[3] (i) GCOS 2016 Implementation Plan; (ii) http://climatemonitoring.info/home/terminology/
[4] http://climatemonitoring.info/home/terminology/ (the ICDR definition was endorsed at the 9th session of the joint CEOS/CGMS Working Group Climate Meeting on 29 March 2018)

2. Algorithm overview

RO data may potentially have benchmarking quality for climate analyses because of the all-weather capability of the technique and because there is no need for calibration (as opposed to many other remote sensing instruments). However, RO processing is generally complex, not the least because different RO missions have different problems (such as low SNR, poor L2 tracking, data gaps, spikes, etc). Thus, besides the processing steps that can be easily described by equations, it is necessary to also have algorithms that can cope with a number of problematic issues. The algorithms in the Radio Occultation Processing Package (ROPP) have been developed over many years to do just that.

ROPP contains a pre-processor module designed to compute ionospheric corrected bending angle, refractivity, and dry temperature profiles either from excess phase or L1 and L2 channel bending angle data derived from radio occultation measurements. A flow chart illustrating the ROPP pre-processor module is given in Figure 2.1. The main aspects of the algorithm for the Level 1B bending angles are described in the ROPP pre-processor user guide [RD.1].

The algorithm description in this ATBD complements the ROPP user guide by focusing on details not described in the user guide or elsewhere. References to equations and sections in the user guide are provided when appropriate. Many of the algorithms in the ROPP pre-processor module are also described in [RD.2]. References to original work on which algorithms are based are provided in the relevant sections.

In the descriptions in Section 3.2, the specific choices of parameters that affect the outcome of the processing are mentioned, such as filter widths, vertical grids, parameters determining specifics in the processing, interpolation methods, etc. The values mentioned are either hard-coded in the software or set in a configuration file in the ROM SAF processing. Although these choices have influence on the results, and contribute to the structural uncertainty of the products, they are not considered to have any negative impact on the products and they do not compromise the benchmarking quality of the data.

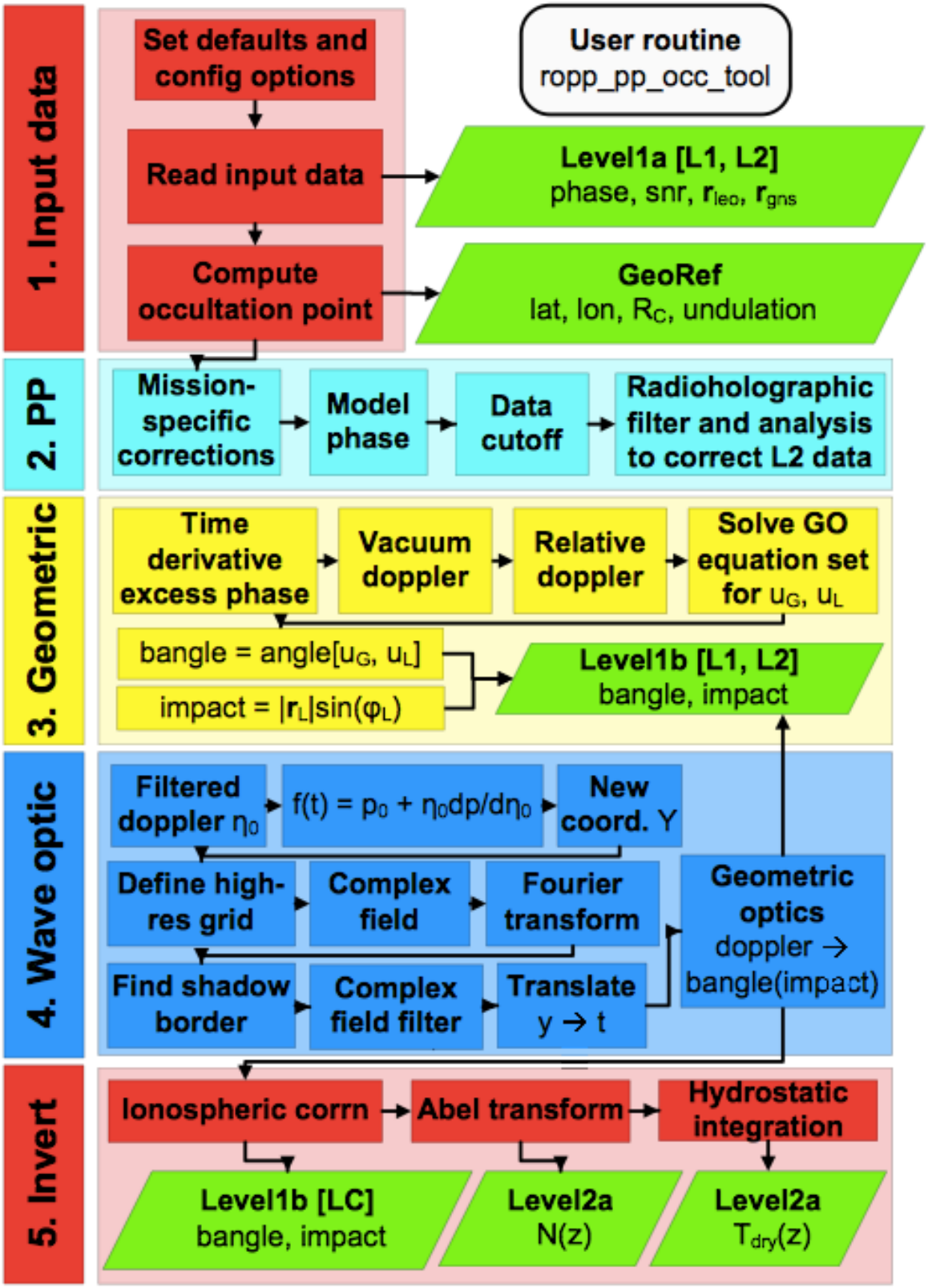

Figure 2.1 Flow chart illustrating calling tree of the ROPP pre-processor occ tool to compute ionospheric corrected bending angle, refractivity, and dry temperature profiles from input L1 and L2 channel amplitude and phase measurements [RD.1].

3. Algorithm description

3.1 Physics of the problem

3.1.1 Fundamental observables

The fundamental observables measured by an RO instrument are the phase, L_i, and amplitude, A_i, of the Doppler-shifted incoming signal. Index i denotes one of the two GNSS frequencies, L1 (f_1 = 1575.42 MHz) and L2 (f_2 = 1227.60 MHz). Each occultation measurement is a time-series of measured phases and amplitudes as well as precise position information for the transmitter (GNSS) satellite and the receiver (LEO) satellite.

3.1.2 Setting and rising occultations

Occultations may be either setting or rising depending on whether the transmitting GNSS satellite "rises" or "sets" as seen from the receiving LEO satellite. In a setting occultation the signal is acquired at very high altitude (~100 km), tracked as the signal path descends into the atmosphere, and eventually lost. Often loss of signal occurs when the terrestrial surface gets in the way, but it may happen earlier. In a rising occultation the signal is acquired when the signal path is in the troposphere and tracked as it rises out of the atmosphere. In principle the two situations are symmetric and the signal processing steps are identical but in practice setting occultations usually deliver higher-quality data in the lower troposphere as the LEO satellite is tracking an already-acquired signal. In contrast, in a rising occultation the signal must be first acquired while traversing the dense and possibly turbulent lower troposphere, which may lead to weak and/or fluctuating signals.

3.1.3 Tracking and sampling the signals

RO-receivers sample the GNSS signal at frequencies that are many orders of magnitude lower than the inherent electromagnetic frequency of the signal. Typical sampling frequencies are 50 Hz or, for GRAS raw sampling, 1 kHz. In contrast the signal frequency is more than 1 GHz. Therefore a million or more electromagnetic cycles pass between each measurement. In order to monitor the accumulated phase (which is necessary in order to derive the Doppler shift), one must be certain to count the number of cycles that have passed correctly, avoiding cycle slips. The standard approach is to track the signal in the so-called closed-loop (CL) mode. The closed-loop approach works well as long as there are no sharp gradients in the atmospheric refractivity. In the lower troposphere, however, higher density, turbulence and sharp changes in humidity may make closed-loop tracking difficult. Therefore many RO-receivers are capable of switching to a different mode where signal phase is just passively monitored at a certain sampling frequency. Examples are the COSMIC satellites' 50 Hz open-loop (OL) mode and the 1 kHz raw sampling (RS) mode of the GRAS receivers [RD.3]. These modes are used only below a certain altitude and make it possible to fully capture the dynamics of the signal in the lower troposphere. A technical description of open-loop tracking can be found in [RD.23]. However, while open loop or raw sampling is active, closed-loop tracking is stopped (though perhaps with some minor overlap between the two modes). Current receivers track only the L1 signal in open loop or raw sampling mode, not the L2 signal, and thus the L2 signal is not tracked at all in the lower troposphere (see specifics for Metop in [RD.25]). Therefore, to perform the ionospheric correction (see below), it is necessary to extrapolate the L2 signal to lower altitudes where the L1 signal is still tracked. This is done as part of the processing. Typical

input data to the processing will therefore consist of a closed-loop data record of L1 and L2 phases and amplitudes, and a separate, partly overlapping open-loop or raw sampling data record of the L1 phase and amplitude.

3.1.4 Correction for navigation bits

GNSS signals are encoded with so-called "navigation bits", an encoded sequence of $\pm\pi$ phase jumps that are effectively random from the perspective of RO data processing. These phase jumps must be identified and corrected for in data processing. This may happen either by recourse to a separately recorded "external" navigation bit sequence received from ground stations (that monitored the same GNSS signal), or by deriving an "internal" navigation bit sequence by direct analysis of the received signal.

3.1.5 Doppler-shift and derived quantities

The received signal is Doppler-shifted due to the motion of the transmitter and receiver satellites. With known satellite positions and velocities this Doppler-shift may be calculated to high precision for the vacuum case. When the ray bends in the atmosphere the angles between the ray path and the directions of motion are slightly different than in the vacuum case, both for the transmitting and the receiving satellite. This leads to a slightly different Doppler-shift. From observed signal phases, the observed Doppler-shift may be found and from this (with precise knowledge of the satellite positions and velocities) the bending of the ray path through the atmosphere may be derived. This leads to a profile of bending angle as a function of impact parameter. The impact parameter is the distance from the centre of refraction to either of the two ray asymptotes as the ray enters or exits the atmosphere.

3.1.6 Ionospheric correction

The bending of a ray passing through the atmosphere consists of a contribution from free electrons in the ionosphere, and a contribution from neutral species in the denser stratosphere and troposphere. The ionospheric contribution has a well-understood dependence on frequency whereas the neutral-atmospheric bending is approximately the same for the L1 and L2 frequencies. Therefore, the presence of both the L1 and L2 signals allows one to disentangle the ionospheric contribution from the ionosphere-free or neutral-atmosphere contribution to the bending. The neutral-atmosphere contribution is the signal of interest in the present application, but in principle the algorithm also delivers the ionospheric signal as output.

3.2 Mathematical description of the algorithm

Given measurements of L1 and L2 excess phases and amplitudes[5] as a function of time, as well as orbits and navigation bits at the sampling times, the following subsections describe the steps taken to obtain the L1, L2, and ionospheric corrected (LC) bending angles as a function of impact parameter.

[5] Due to a problem with the open loop 50 Hz amplitude SNRs provided by the EUMETSAT Secretariat, the open loop 50 Hz amplitude SNRs used as input to the ROM SAF processing for Metop are reconstructed from the 1 kHz raw sampling data.

3.2.1 Coordinate transformation

The LEO and GNSS positions are converted from an Earth Centered Inertial (ECI) frame to an Earth Centered Fixed (ECF) frame. For Metop this includes an intermediate transformation from the J2000 ECI frame to the so-called True-of-Date ECI frame using formulas in [RD.27]. The Greenwich Mean Sidereal Time (GMST) angle at each measurement epoch is calculated and the position vectors are rotated accordingly.

3.2.2 Ellipsoidal correction

Based on the LEO and GNSS orbits in the ECF frame, the straight-line tangent point (SLTP) relative to the Earth's center is calculated for all samples of the occultation. The coordinates of the SLTP are transformed to geodetic latitude, longitude, and altitude above the ellipsoid. A single reference location is taken as the geodetic latitude and longitude of the SLTP on the line for which the absolute value of the SLTP altitude is the smallest. In the following this SLTP is called the reference SLTP.

The reference azimuth is calculated as the angle between the reference meridional plane (the plane containing the Earth's center, the North pole, and the reference SLTP) and the reference occultation plane (the plane containing the Earth's center and the GNSS and LEO satellite positions corresponding to the reference SLTP). The angle is defined to be positive between 0 and 360, counted clockwise from the North towards the GNSS-to-LEO direction.

The Earth's radius of curvature in the occultation plane at the reference location is calculated based on the azimuth angle using theorems of Meusnier and Euler [RD.4]. The center of curvature is obtained as the difference between the vector corresponding to the reference location on the Earth's ellipsoid and a vector having the length of the radius of curvature and the direction of the local normal to the ellipsoidal surface.

The center of curvature is subtracted from the satellite positions in subsequent processing involving the satellite orbits.

3.2.3 Computation of satellite velocities

The input LEO and GNSS satellite positions and velocities are provided at the measurement times. However, the velocities are not used in the ROPP processing. Instead, satellite velocities are repeatedly (when needed) calculated by fitting a 5th order polynomial to the satellite positions (for each Cartesian component) over the time span of the occultation. The positions given by the 5th order polynomial and the velocities based on the derivative of the polynomial are used in the ROPP processing at various subsequent stages, including the calculation of bending angles.

3.2.4 Data cut-off

To avoid measurements corrupted by signal tracking errors, data are cut short from below (end of setting occultations; beginning of rising occultations) if the L1 amplitude is not larger than a certain threshold. The threshold value is set to zero for all missions, i.e, data are only cut short if the L1 amplitude in the lowest part of the occultation is zero (cf. Section 3.3.3 in [RD.1]). For CHAMP and GRACE processing, data are additionally cut short if tracking errors are detected in the L1 phase. The detection is based on analysis of

the difference between the L1 excess phase and an excess phase model. The second derivatives over 1-second intervals are computed and data are cut short if the second derivative exceeds 2 m/s^2. Likewise, data are cut short for all missions if a smoothed version of the L1 bending angle computed by geometrical optics (GO) (cf. Section 3.2.14) and with monotonized impact parameters (cf. Section 3.2.19) exceeds a threshold at the bottom or top of the profile. The threshold is 0.1 rad. A bending angle larger than 0.1 rad is allowed as long as it is not at the end points of the profile. It should be noted that the smoothed version of the bending angle is only used to cut out large tracking errors if there are some; data in the troposphere are processed using wave optics (WO) (cf. Section 3.2.15).

3.2.5 Application of navigation bits

If navigation bits are available and not already applied by the data provider (EUMETSAT or UCAR), a check is made to see if the provided navigation bits are consistent with the observed phases and amplitudes. If the correlation is deemed adequate, the data is corrected using the input navigation bit record. If not, ROPP internal navigation bits from analysis of the recorded phases and amplitudes are calculated by identifying phase jumps of π radians. The navigation bit record is then used to correct the observed phases and amplitudes. This is only done for COSMIC. For CHAMP and GRACE, navigation bit correction is not required, and for GRAS data, the navigation bits are already applied by the data provider, and navigation-bit corrected excess phases are provided at 50 Hz. If necessary (for data provided by EUMETSAT), the OL and CL data records are merged whenever the two records overlap.

3.2.6 Handling of data gaps

Metop data contain significant amounts of data gaps [RD.3, RD.5, RD.25]. Before the firmware upgrade to the Metop satellites in 2013, about 30% of all rising occultations were affected by gaps in closed-loop data and most occultations were affected to some degree by small gaps in the raw sampling data. Improved onboard software has reduced the number of gaps to a much lower level, but they will always be present in the already acquired data and so finding a good way to handle data gaps in the data processing is important.

In the processing, the lengths of the gaps are identified, and if a gap is shorter than a set threshold, the gap is filled in by linearly interpolating the amplitude as well as the deviation of the excess phase from a phase model. The phase model is based on the MSIS climatology [RD.6] combined with a simple humidity model [RD.7]. The relative humidity is assumed to be 90% below 15 km and zero above 15 km. If the gap is longer than the threshold, the data after the gap is rejected for setting occultations, the data before the gap is rejected for rising occultations. The gap length cutoff is set to 0.8 s. The parameter called ‘Lost Carrier Flag’ holds track of the data gaps smaller than 0.8 s and is included in the output.

3.2.7 Computation of excess phase model

A model of the excess phase as a function of impact parameter is computed based on a model of the bending angle and the satellite orbits. The model of the bending angle is based on the MSIS90 climatological model [RD.6] in combination with an assumption of 90% humidity (Q) below 15 km (cf. Section 3.3.1 in [RD.1]). The MSIS+Q bending angle

profile is extended downward (if necessary) by linear extrapolation of log(BA) to cover the span of the occultation.

3.2.8 Computation of refractive L2 amplitude

Assuming that L2 data in general may be degraded, the L2 amplitude is replaced by a smooth GO amplitude using the satellite orbits and the impact parameter levels of the excess phase model [RD.7] (see also Section 3.3.5 in [RD.1]). The amplitude is normalized so that the mean between 30 and 35 km is equal to that of the L1 CA amplitude. This L2 amplitude is further modified later in the processing (see below).

3.2.9 Correction of L2 cycle-slips

The measured L2 excess phase is re-accumulated using the excess phase model to correct for cycle-slips (should such exist).

3.2.10 Radio holographic filtering

A radio holographic filter is applied to the corrected L2 data following the approach in [RD.9, RD.26] (cf. Section 3.3.5 in [RD.1]).

Before the filtering, a reference L2 excess phase is computed based on the impact parameter from a radio holographic spectral analysis.

The reference excess phase is subtracted from the corrected L2 excess phase, and a complex signal is formed using the computed refractive L2 amplitude. A Fourier filter with a window corresponding to about 500 m is applied to the complex signal. The accumulated phase of the filtered signal is computed and the reference phase is added back on to obtain the filtered L2 excess phase.

3.2.11 Weighting functions and badness score

A quality control indicator, Q_{L2}, is computed as described in [RD.7] and [RD.1] (Eq. 3.6 in the latter). It is based on impact parameters and their RMS deviation obtained from a radio holographic analysis of the excess phase and amplitude (corrected excess phase and amplitude in case of L2). The maximum impact parameter (p_C) below about 20 km, for which Q_{L2} exceeds a value of 25, is identified, and a weighting function used later for modification of L2 excess phase and amplitude is based on this impact parameter. The so-called "L2 badness score" is defined as the maximum of Q_{L2} between 25 and 50 km. It is an output diagnostic and is used as a quality control measure.

3.2.12 Modification of L2 amplitude

The L2 amplitude (as corrected in previous steps) is reduced to 10% of its value below p_C by applying a weighting function [RD.7]. The transition zone from large to small amplitude is about 2 km.

3.2.13 Modification of L2 excess phase

The L2 excess phase (as corrected in previous steps) is smoothed using a sliding polynomial filter of degree three, and with a window corresponding to about 250 m. As described in [RD.7], the filtering is applied to the difference between the L2 excess phase and the excess phase model.

Below p_C, the L2 excess phase is replaced by the L1 excess phase plus a smooth estimate of the L1 and L2 excess phase difference. The L1-L2 excess phase difference below p_C is estimated in the following way: Based on the satellite orbits and the impact parameters from the radio holographic analysis mentioned in Section 3.2.10, the mean bending angle difference in a 2 km range just above p_C is computed. This difference is used to find an almost linearly varying excess phase difference. The replacement of the L2 excess phase is applied via a transition in the Doppler shift around p_C using a weighting function (cf. Eqs. 2.9–2.11 in [RD.1]). The transition zone is about 2 km.

Finally, up to three single outliers (click removal) in the L2 excess phase are removed (should such exist) and replaced by the mean of the two neighboring samples. In case of no outliers, the L2 excess phase is hardly altered. The final result is the L2 excess phase that is used later in the GO- and WO processings.

3.2.14 Geometrical optics processing (above 25 km)

Geometrical optics is used to calculate the L1 and L2 bending angles as a function of impact parameter above 25 km. Given the geometry of the problem and the parameters defined in Figure 3.1, the principal equation relating the measured Doppler-shift, D (in units of m/s), to the bending angle and impact parameter can be written as

$$D = \mathbf{v}_L \cdot \mathbf{u}_L(a) + \mathbf{v}_G \cdot \mathbf{u}_G(a),$$

where $a = p_L = p_G$ is the asymptotes' common impact parameter in line with the assumption of spherical symmetry. For the impact parameter, a, that fulfills this relation, the angle between the two unit vectors (π - α) determines the bending angle. Technically, the problem can be solved in different ways. In ROPP it is solved (iteratively) setting up a non-linear set of equations (Eqs. 2.19-2.22 in [RD.1])[6] involving the satellite orbits and the excess Doppler-shift (the measured Doppler-shift minus the vacuum Doppler-shift).

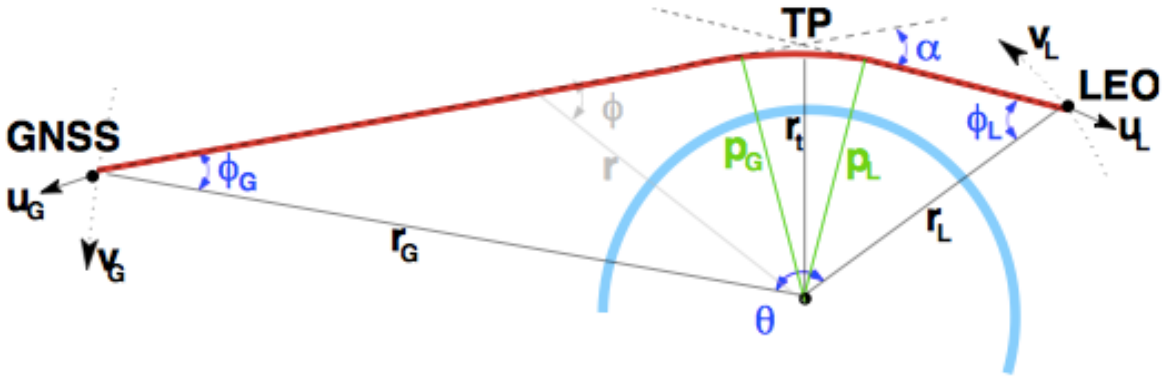

Figure 3.1 Radio occultation geometry. Shown are the bending angle (α), the GNSS and LEO side impact parameters (p_G, p_L), the GNSS and LEO coordinate vectors (r_G, r_L), the ray path (solid red line) and the satellite side asymptotes of the ray path (dashed). The vectors $\mathbf{u}_G$ and $\mathbf{u}_L$ denote unit vectors along the asymptotes, whereas $\mathbf{v}_G$ and $\mathbf{v}_L$ are the satellite velocities projected onto the occultation plane. Radius r_t shows the radial distance between the centre of curvature and the ray tangent point [RD.1].

[6] Though see limitation in Section 5.2.6

Before the calculation of bending angles, the excess phase is de-trended using spline regression of the logarithm of the phase, and the de-trended excess phase is then smoothed using a sliding polynomial filter with a window corresponding to about 3 km. The calculation of the excess Doppler shift is given by the sum of the derivative of the sliding polynomial and the derivative of the trend [RD.7].

3.2.15 Canonical Transform (CT2)

The Canonical Transform of the second kind (CT2) is used in the calculation of the L1 and L2 bending angles below 25 km. The approach follows that of [RD.10], involving a Fourier Integral Operator (FIO) to obtain a complex field as a function of impact parameter. The main steps are also described in [RD.1] (Section 2.3.3 therein). The CT2 is performed on both L1 and (corrected) L2 signals.

3.2.16 Filtering and smoothing

The complex field obtained from the FIO is smoothed using a Fourier filter. Before the application of the Fourier filter, the complex field is multiplied by a reference field to compress the spectral width. The reference field is based on a phase model obtained from the FIO phase by a sliding polynomial filter of degree three, and a window width of 250 m. The Fourier filter is also applied with a window corresponding to about 250 m. The phase is re-accumulated and the phase model is added back on. This will in the following be referred to as the CT phase. The resulting amplitude is in the following referred to as the CT amplitude. The filtering is done for both L1 and L2 signals.

The CT amplitude is correlated with a step function to obtain the shadow border altitude, p_{min} (different for L1 and L2) [RD.7]. The CT phase is smoothed by a sliding polynomial filter of degree three and a variable window. Below p_{min} the window is 1 km, and above it is 2 km. The transition zone is about 2 km wide.

A radio holographic analysis is performed to determine the bending angle error from the spectral width of the complex wave field (Eqs. 3.7–3.8 in [RD.1]).

3.2.17 Computation of bending angles

The derivative of the CT phase is transformed to the Doppler shift as a function of a new coordinate related to time [RD.10] (time is a multi-valued function of the new coordinate). The bending angle as a function of impact parameter is now solved in the same way as in Section 3.2.14 (using Eqs. 2.19-2.22 in [RD.1]), allowing for the correct solution in multipath zones when there is more than one Doppler shift value at a given time.

The L1 and L2 bending angles are effectively cut off below their respective p_{min} values, and interpolated onto equidistant impact parameter levels below 25 km. The number of equidistant levels is determined by the number of 50 Hz samples below 25 km.

The GO and WO bending angles are merged by applying a simple cosine weighting function between 20 and 25 km (i.e., 100% weight to the WO solution at 20 km, 100% weight to the GO solution at 25 km, and a gradual cosine transition in between).

3.2.18 Extrapolation of L2 bending angle

The L2 bending angle (which does not reach below the L2 p_{min} value) is extrapolated down to the L1 p_{min} value. The extrapolation is based on the mean difference between L1 and L2 bending angles in the range 1–6 km above the L2 p_{min} value, maintaining a constant difference between L1 and L2 bending angles below [RD.7]. In a transition zone from the L2 p_{min} value to 2 km above, the extrapolated solution is merged with the estimated L2 bending angle in this interval by applying a simple cosine weighting function.

3.2.19 Monotonization of impact parameters

The computed bending angle coming out of the GO processing is sometimes, in small intervals, a multi-valued function of the impact parameter. Because a multi-valued function cannot be used for the inversion to higher-level products, a monotonization procedure is applied to the impact parameter profile [RD.12]. At various stages in the processing (e.g., when computing the excess phase model), intermediate versions of impact parameter profiles are monotonised in the following way: Starting from the top index (assuming a setting occultation), impact parameters that are more than 500 m larger than the smallest value so far is set to the smallest value plus 500 m. The resulting impact parameter curve is then enveloped by two monotonic curves, each with a minimum slope of 1% of the mean slope for the whole profile. The mean of these two envelope curves defines the monotonized impact parameter curve. If impact parameters are already monotonic on input, the algorithm leaves the data untouched.

After the WO processing, the final impact parameters are monotonized, practically only affecting the profiles above 25 km where impact parameters might sometimes be non-monotonic (the output from the WO processing is already on monotonic equidistant impact parameter levels).

3.2.20 Un-optimized ionospheric correction

Un-optimized ionospheric-corrected bending angles are computed using the standard linear combination of L1 and L2 bending angles (Eq. 2.39 in [RD.1]), as well as a higher order residual ionospheric correction [RD.31]. In the process, the L2 bending angles are interpolated to the L1 impact parameters. The higher order residual correction is based on a fixed Chapman profile for the ionospheric electron density. The Chapman profile has a scale height of 60 km and the electron density peak is fixed at a radius of 6670 km. The outcome of the ionospheric correction is referred to as the LC bending angle.

3.2.21 Computation of tangent points and azimuth angle

The latitude and longitude of the tangent points are computed as described in [RD.13]. The azimuth angle of the occultation plane for each tangent point location is determined as the angle between the LEO-GNSS straight-line direction and local North at that location. These computations are done with respect to a common center of curvature (cf. Section 3.2.2), and the resulting latitude is the geographic latitude.

3.2.22 Interpolation to common impact parameter levels

The L1, L2, and LC bending angle profiles, as well as latitude, longitude, and azimuth as a function of impact parameter, are linearly interpolated to equidistant impact parameter levels with 100 m in between levels. Latitude, longitude and azimuth angle, together, are

interpolated by transformation to six Cartesian coordinates (two unit vectors) in order to precisely preserve the three-dimensional relation between these three parameters.

3.3 Error sources

As a general consideration, the radio occultation signal consists of an excess phase and an amplitude. High-quality data is data with high SNR both in terms of amplitude and in terms of excess phase.

Amplitude noise is dominated by instrument noise under quiet ionospheric conditions. However, in the presence of ionospheric disturbances, or tilted sporadic E-layers, it can be severely affected by scintillations [RD.22]. Under quiet conditions the SNR is generally high except in the middle to lower troposphere, where the denser atmosphere leads to loss of signal intensity. This is particularly true when the humidity is high, which typically occurs in the tropics [RD.23]. This results in degraded bending angle data quality in the lower to middle troposphere, particularly in the tropics.

Besides instrument noise, the measured excess phase is affected by residual ionospheric noise [RD.24]. The ionospheric contribution to the signal is not fully removed by the ionospheric correction due to short timescale ionospheric variation and other higher order effects not accounted for in the residual correction. Since the measured excess phase signal is a function of atmospheric density it falls off approximately exponentially with impact height and so the noise comes to dominate the signal at high altitudes in the upper stratosphere and above. In the lower troposphere the tracking of the L2 signal becomes difficult and for that reason only the L1 signal is useful. This limits the accuracy of derived products.

The highest data quality is therefore found at intermediate altitudes of the higher troposphere to lower stratosphere, where the signal is strong both in terms of amplitude and in terms of excess phase.

4. Practical considerations

4.1 Validation method

As a whole, the algorithms are used to process a number of occultation observations, which are then compared to the corresponding profiles extracted from ECMWF analyses and forecasts (forward modelled to bending angle as a function of impact parameter). The bending angles are also compared to the corresponding bending angles produced by EUMETSAT and CDAAC.

Many parts of the algorithms described here together with those described in [RD.14] and [RD.15], have been validated over many years, as similar versions of the algorithms have been used to produce results for scientific publications and reports (see [RD.2], [RD.7], [RD.9], [RD.12], [RD.20], [RD.21], [RD.25], [RD.26], [RD.29], and [RD.30]).

4.2 Quality control and diagnostics

The following quality control parameters are used to ensure the quality of the bending angle products[7]:

L2 quality score:

Measures the quality of the L2 signal. This score is defined as the maximum of an L2 penalty function over the interval 25–50 km (see [RD.10]). The L2 quality score is constructed such that a low value means high quality data. It is generated in the code when the relevant parameters are readily available and is output together with the data.

Besides checking the above quality control parameters, the following sanity checks are made to the data themselves:

- The independent variable (impact height) is required to vary monotonously.
- The bending angle is required to have valid values above and below certain impact heights (e.g., above 60 km and below 20 km).
- At very high altitudes (e.g., above 60 km), the optimized bending angle is required to be within a certain threshold of the background profile used for statistical optimization (cf. [RD.14]).
- The bending angle is compared to the corresponding profile extracted from an NWP model (forward modeled to bending angle).

The bending angle is marked as non-nominal if any of the above checks results in parameters or data values outside defined thresholds. The bending angle is also marked as non-nominal if the incoming excess phase was marked as non-nominal, or if the processing to refractivity results in non-nominal refractivity [RD.14].

[7] Explicit numbers for the QC settings can be found in the validation reports at www.romsaf.org/product_documents.php

4.3 Outputs

The output of the processing to bending angle is a ROPP NetCDF file containing the following profile variables:

- Latitude
- Longitude
- Azimuth
- L1 bending angle
- L2 bending angle
- LC bending angle
- Impact parameter

The same NetCDF file contains the output from the refractivity [RD.14] and dry temperature [RD.15] processing. A more complete and technical description of the output to the NetCDF file can be found in [RD.16].

The above-mentioned variables are also written to a BUFR file [RD.17].

5. Assumptions and limitations

5.1 Assumptions

5.1.1 Spherical symmetry

Radio occultation data are generally processed under the assumption of spherical symmetry. However, in principle this is only an apparent assumption because it depends on the interpretation of the retrieved profiles. If profiles are interpreted as representing the vertical structure in the atmosphere at a given fixed location, then the spherical symmetry assumption gives rise to a real error because the atmosphere is only approximately spherically symmetrical. If, on the other hand, retrieved profiles are interpreted as being weighted averages of the 3-dimensional (3D) atmosphere (primarily in the 2-dimensional (2D) occultation plane), the spherical symmetry assumption does not in principle give rise to any errors. This is why it could be an advantage to assimilate occultation data with 2D or 3D observation operators. A 2D observation operator for bending angle assimilation has been developed in [RD.18].

5.1.2 Geometrical optics approximation

Above 25 km, bending angles are derived using geometrical optics, i.e., the assumption that there is only one ray path between the transmitter and the receiver at any given time. This assumption may not hold for very sharp vertical stratospheric gradients, but such cases are probably rare. More likely, and not uncommon, very sharp ionospheric gradients may generate multipath interference and result in very strong scintillations. In such situations there are multiple ray paths between the transmitter and the receiver, and the derivation of the bending angle by differentiation of the Doppler shift is flawed and results in a non-monotonic impact parameter sequence. Usually the smoothing that is applied at various stages of the processing mitigates the situation, and the monotonization (cf. Section 3.2.19) ensures a monotonic impact parameter in the end.

5.1.3 Assumptions in wave optics

Wave optics (WO) processing (below 25 km) resolves the multipath, but is in itself based on a number of assumptions that may not always hold [RD.28]. The processing by WO usually results in more noise than GO processing. The reason for this can probably be attributed to the violation of some of these assumptions in practice. In rare cases, strong horizontal gradients and multipath in combination, results in a partial breakdown of the WO solution [RD.19].

5.2 Algorithm limitations

The following subsections discuss limitations in the algorithms described in the corresponding subsections with the same titles in Section 3.2.

5.2.1 Coordinate transformation

The orbits from the COSMIC Data Analysis and Archival Center (CDAAC) are in an Inertial True-of-Epoch (ITOE) coordinate frame, which is approximately, but not exactly, equal to the ECI frame assumed in the rotation in ROPP. It is not clear how this affects the retrievals, but possibly the effect is minor.

Since the GNSS orbits are given at the time of signal transmission, whereas they are tagged to the time of signal reception (and because it is the signal reception time that determines the GMST angle in ROPP), they are slightly incorrectly rotated. The incorrect treatment of the GNSS orbits is judged to have very little influence on the retrievals. An alternative and more transparent approach (though not implemented in ROPP) would be to do the retrieval in the ECI frame, and only calculate the GMST angle to get the correct longitude of the occultation tangent points.

5.2.2 Ellipsoidal correction

It should be noted that the transformation of the SLTP to geodetic latitude, longitude, and altitude above the ellipsoid is approximate. However, since it is the SLTP closest to the surface of the ellipsoid that is used to determine the center of curvature, the approximation is small. The altitude for the SLTP closest to the surface is typically less than 100 m above the ellipsoid, and the error in the reference location on the surface is thus judged to be much less than 100 m.

5.2.3 Computation of excess phase model

The bending angle as a function of impact parameter is used to find the model Doppler shift, which in turn is used to find the model excess phase. However, the computation of the Doppler shift in ROPP uses formulae (e.g., Eq. 2.17 in [RD.1]), which implicitly assume that the GNSS satellite velocity going into the formulae is the actual velocity at the time of transmission. On the other hand, the GNSS satellite velocity is calculated in ROPP as the derivative of the position at transmit time with respect to the reception time (cf. Section 3.2.3). This is not the actual velocity, but can be considered an apparent velocity (the velocity as seen from the LEO). Thus, there is an inconsistency between the way the GNSS satellite velocities are calculated in ROPP and the way they are used in some places in ROPP. The formula for the Doppler shift (correctly given in, e.g., [RD.8]), when the GNSS satellite velocity is the apparent one, is different from those used in ROPP. The difference is almost constant and on the order of 10 mm/s. This is much larger than the anticipated velocity accuracy. Appendix B in [RD.11] outlines the derivation of formulae for the Doppler shift showing the results for the two different interpretations of the GNSS velocity. In the following, the formulae used in the ROPP software will be referred to as "incorrect", although it could be argued that they are correct, and that it is the GNSS satellite velocity going into the formulae that is incorrect.

In most parts of the ROPP software, both the atmosphere-free Doppler shift and the expected Doppler shift due to the bending (Eq. 2.17 in [RD.1]) are calculated using the incorrect formula, and when subtracted from each other, the error mostly cancel. However, in the computation of the excess phase model, the range between the satellite positions is subtracted from the integrated Doppler shift (Eq. 3.2 in [RD.1]). The result is that the excess phase model has a tilt of about 10 mm/s. The tilt is easily seen in the upper part of occultations where the excess phase model is supposed to be nearly horizontal (see, e.g., Figure 2.2 in [RD.11]).

Possibly the effect of the tilt on later results is very small or non-existent, since the excess phase model is used only as a reference subtracted from the measured signal during correction and filtering, for which an accuracy of about 10 Hz should be sufficient.

5.2.4 Radio holographic filtering

The L2 reference phase is calculated using the incorrect formula for the Doppler shift (cf. Section 5.2.3) resulting in a tilt in the reference excess phase relative to the measurement.

5.2.5 Modification of L2 excess phase

The smooth excess phases calculated to estimate the L1-L2 excess phase difference are tilted by about 10 mm/s because of the above-mentioned issue (cf. Section 5.2.3), but only their difference is used, and the errors largely cancel.

5.2.6 Geometrical optics processing (above 25 km)

The use of incorrect Doppler shift formulae (cf. Section 5.2.3) to solve for the bending angle is insignificant, since both the expected atmosphere-free Doppler and the relation between bending angle and Doppler shift are computed using the incorrect formulae, and the errors largely cancel. In particular, it can be shown that the error is less than 1 mm/s in the troposphere, and proportional to the bending angle (i.e., falls off exponentially above).

6. Description of differences for NRT, offline, CDR and ICDR products

This chapter describes the parts of the algorithm which are different for NRT, offline, CDR and ICDR products.

6.1 NRT

N/A

6.2 Offline

The algorithms used in offline are the ones described in Chapter 3.

6.3 CDR

The algorithms used for the CDR products are the same as the algorithms used in offline, except for the residual ionospheric correction described in Section 3.2.20.

6.4 ICDR

The algorithms used for the ICDR products are the same as the algorithms used for the CDR products.

Appendices

A.1 Description of how to run the code

The code is run by the following command:

```
ropp_pp_occ_tool <input_file> --no-ranchk -o <output_file> -c
<config_file>
```

The input file is a ROPP NetCDF file containing high-resolution Level 1A data. The output file is a ROPP NetCDF file containing high-resolution Level 1B and 2A data.

The generation of a BUFR file is done by the following commands:

```
ropp2ropp <input_file> --no-ranchk -o <output_file> -p
<thin_file>
ropp2bufr <input_file> -o <output_file>
```

The input file to the `ropp2ropp` command is a ROPP NetCDF file containing Level 1B and 2A data (the high-resolution output of the retrieval). The output file of the `ropp2ropp` command is a ROPP NetCDF file containing thinned Level 1B and 2A data. The thinning file is the one provided by EUMETSAT (`ropp_thin_eum-247.dat`). The input file to the `ropp2bufr` command is the NetCDF file containing thinned Level 1B and 2A data and the output file is a BUFR file.

A.2 Configuration file

An example of a ROPP PP configuration file is given below. The values of parameters are not necessarily the final ones that will be set in the offline and reprocessing of bending angles.

```
# $Id: $

#****c* Configuration Files/metop_pp.cf *
#
# NAME
#    metop_pp.cf - METOP data configuration file for pre-processor
#    implementations in ROPP
#
# SYNOPSIS
#    <pp_program> ... -c metop_pp.cf ...
#
# DESCRIPTION
#    This file reflects the configuration for the PP
#    implementations within ROPP suitable for use with METOP data.
#
# NOTES
#
# AUTHOR
#   Met Office, Exeter, UK.
#   Any comments on this software should be given via the ROM SAF
#   Helpdesk at http://www.romsaf.org
#
# COPYRIGHT
#   (c) EUMETSAT. All rights reserved.
#   For further details please refer to the file COPYRIGHT
#   which you should have received as part of this distribution.
```

```
#
#****

#-------------------------------------------------------------------------------
# 0. Output options
#-------------------------------------------------------------------------------
output_lev1a = .false.      # Flag to output (modified) level 1a data

output_lev1b = .true.       # Flag to output level 1b data

output_lev2a = .true.       # Flag to output level 2a data

output_diag  = .true.       # Flag to output additional diagnostics

#-------------------------------------------------------------------------------
# 1. Excess phase to bending angle processing
#-------------------------------------------------------------------------------

# 1.1 Occultation processing method
# ---------------------------------

# GO - use GEOMETRIC OPTICS processing to derive bending angle as a function of
#      impact parameter from excess phase as a function of time.
# WO - use WAVE OPTICS (CT2 algorithm) processing to derive bending angle as a
#      function of impact parameter from excess phase as a function of time.

occ_method = WO

# 1.2 Filtering method
# --------------------

# optest - use OPTIMAL ESTIMATION: solution of integral equation
# slpoly - use SLIDING POLYNOMIAL

filter_method = slpoly

# 1.3 Smoothing bending angle profile
# -----------------------------------

fw_go_smooth = 3000.0  # Filter width for smoothed GO bending angles (m)

fw_go_full = 3000.0    # Filter width for full resolution GO bending angles (m)

fw_wo = 2000.0         # Filter width for wave optics bending angle above 7 km (m)

fw_low = -1000.0       # Filter width for wave optics bending angle below 7 km (m)

# 1.4 Maximum height for wave optics processing
# ---------------------------------------------

hmax_wo = 25000.0      # Maximum height for wave optics processing (m)

# 1.5 Data cut-off limits
# -----------------------

Acut     = 0.0         # Fractional cut-off limit for amplitude

Pcut     = -2000.0     # Cut-off limit for impact height

Bcut     = 0.1         # Cut-off limit for bending angle

Hcut     = -250000.0   # Cut-off limit for straight-line tangent altitude

# 1.6 CT2 options
# ---------------

CFF      = 3           # Complex field filter flag (CFF = 'Pa')

dsh      = 200.0       # Shadow border width (m)

# 1.7 Degraded L2 data flag
# -------------------------

opt_DL2  = .true.
```

```
# 1.8 Compute and output spectra flag
# -----------------------------------

opt_spectra = .false.

# 1.9 Paths to EGM96 geoid model coefficients and corrections file
# ----------------------------------------------------------------

egm96 = ../data/egm96.dat                 # EGM96 coefficients file

corr_egm96 = ../data/corrcoef.dat         # Correction coefficients file

#-------------------------------------------------------------------------------
# 1. Ionospheric correction processing
#-------------------------------------------------------------------------------

# 1.1 Ionospheric correction method
# ---------------------------------

# GMSIS - use MSIS climatology bending angle (searching global MSIS profiles
#         for best fit profile to obs) in ionospheric correction,
#         statistical optimization and bending angle to refractivity inversion.
#
# MSIS - use MSIS climatology bending angle in ionospheric correction,
#        statistical optimization and bending angle to refractivity inversion.
#
# GBARO - use BAROCLIM bending angle (searching global BAROCLIM profiles
#         for best fit profile to obs) in ionospheric correction,
#         statistical optimization and bending angle to refractivity inversion.
#
# BARO - use BAROCLIM bending angle in ionospheric correction,
#        statistical optimization and bending angle to refractivity inversion.
#
# BG   - use climatology from a specified input file containing
#        background temperature, pressure and humidity
#        (e.g. from an NWP analysis). The input filename can be specified
#        using the '-bfile' command line argument or setting 'bfile' (see 1.5).
#
# NONE - linear combination of L1 and L2 bending angles in ionospheric
#        correction, no additional information above observed profile top
#        in the inverse Abel to compute refractivity.

method  = GBARO                # Ionospheric correction method

# 1.2 Abel integral method
# ------------------------

# LIN  - assume linear variation of bending angle and ln(n) between
#        observation levels. This algorithm is used in ROM SAF NRT processing
#
# EXP  - assume exponential variation of bending angle and ln(n) between
#        observation levels. This algorithm is used in ropp_fm module.

abel = LIN

# 1.3 Statistical optimisation method
# -----------------------------------

# SO  - statistical optimisation.
# LCSO  - linear combination plus statistical optimisation.

so_method = so

# 1.4 Climatology model coefficients files
# ----------------------------------------

msisfile = ../data/MSIS_coeff.nc           # MSIS coefficients file for phase model
mfile    = ../data/BAROCLIM_coeff.nc       # Model coefficients file for stat. opt.

# 1.5 Background model temperature, humidity, pressure file
# ---------------------------------------------------------

bfile    = BG_file.nc       # Background meteorology profile file (method=BG)
```

```
#------------------------------------------------------------------------------
# 2. Impact parameter grid
#------------------------------------------------------------------------------

# The ionospheric correction interpolates L1 and L2 bending angle profiles onto a
# standard grid.

dpi = 100.0            # Step of standard impact parameter grid (m)

#------------------------------------------------------------------------------
# 3. Smoothing bending angle profile
#------------------------------------------------------------------------------

# A smoothed bending angle profile is derived compute the fit of observed bending
# angles to the model bending angle profile.

np_smooth = 3          # Polynomial degree for smoothing regression

fw_smooth = 1000.0       # Filter width for smoothing profile

#------------------------------------------------------------------------------
# 4. Model bending angle profile fit to observations
#------------------------------------------------------------------------------

# To avoid systematic deviations from the observed profile with climatology,
# the model profile is scaled to the observed profile by a fitting method.

sf_method = regular     # Search and fit method (convoluted or regular)

nparm_fit = 2           # Number of parameters for model fit regression

hmin_fit  = 40000.0     # Lower limit for model fit regression

hmax_fit  = 60000.0     # Upper limit for model fit regression

omega_fit = 0.3         # A priori standard deviation of regression factor

#------------------------------------------------------------------------------
# 5. Ionospheric correction and statistical optimization
#------------------------------------------------------------------------------

# The method described by Gorbunov (2002) is implemented to perform ionospheric
# correction with statistical optimization.

f_width = 50.0         # Ionospheric correction filter width

delta_p = 100.0               # Step of homogeneous impact parameter grid

s_smooth = 50.0               # External ionospheric smoothing scale

z_ion = 50000.0               # Lower height limit of ionospheric signal

z_str = 35000.0               # Lower height limit of stratospheric signal

z_ltr = 12000.0               # Lower height limit of tropospheric signal

n_smooth = 11          # Number of points for smoothing (must be odd)

model_err = 0.5        # A priori model error std.dev. (dyn.est. if negative)

opt_XL2  = .false.       # L2 extrapolation on optimized bending angles

#------------------------------------------------------------------------------
# 6. Bending angle inversion to refractivity
#------------------------------------------------------------------------------

# The Abel inversion is computed to retrieve refractivity from corrected
# bending angles. The corrected bending angle profile is extended
# using MSIS or BAROCLIM data above the observed profile top.

ztop_invert = 150000.0 # Height of atmosphere top for inversion

dzh_invert = 50.0      # Step of inversion grid above observation top
```

```
dzr_invert = 20000.0   # Interval for regression in inversion

#-------------------------------------------------------------------------------
# 7. Tangent point lat-lons
#-------------------------------------------------------------------------------

# Set tp_bending=.true. to update lat-lons accounting for bending

tp_bending = .true.
```